Dispersion and distribution of ruthenium on carbon-coated ceramic monolithic catalysts prepared by impregnation

E. Crezee[a], P.J. Kooyman[b], J. Kiersch[c], W.G. Sloof[c], G. Mul[a], F. Kapteijn[a,*], and J.A. Moulijn[a]

[a]*Reactor and Catalysis Engineering, Delft University of Technology, Julianalaan 136, 2628 BL, The Netherlands*
[b]*National Centre for High Resolution Electron Microscopy, Delft University of Technology, Rotterdamseweg 137, 2628 AL Delft, The Netherlands*
[c]*Laboratory of Materials Science, Delft University of Technology, Rotterdamseweg 137, 2628 AL Delft, The Netherlands*

Received 15 July 2003; accepted 5 August 2003

Carbon-coated monolithic catalysts were prepared by dipcoating a cordierite substrate in a Furan resin, after which the ruthenium was incorporated by impregnation with a $[RuCl_5]^{2-}$ complex. Immobilization of the precursor proceeded particularly via weak physisorption. Since the carbon-coated monolithic supports have a broad pore-size distribution, redistribution of the ruthenium precursor occurred upon drying due to capillary forces, resulting in low dispersion. A significant amount of ruthenium is present on the surface of the carbon inclusions located deep in the cordierite walls, making the diffusion path of the reactants to the active ruthenium sites considerably larger than the average carbon-coating thickness. For successful application of the carbon-coated monolithic catalysts in gas–liquid reactions, the deposition of carbon in the walls of the monolith should be prevented and maldistribution of ruthenium upon drying should be solved.

KEY WORDS: monolithic catalyst; ruthenium; carbon-coating; impregnation; dispersion; distribution.

1. Introduction

Carbon has some characteristics that are very valuable and not attainable using any other support. These are the possibilities to tailor the physical/chemical surface properties of the support and to modify the nature of the metal/support interaction. In contrast to most inorganic supports, activated carbons show excellent stability in virtually all liquid media. Furthermore, they allow an easy recovery of the active phase from the catalyst by burning off the support. Carbon is therefore a very attractive carrier to be applied in three-phase (gas–liquid–solid) reaction systems. The use of a fixed-bed reactor with supported metal catalyst eliminates catalyst filtration and improves the economy of the process. Compared to conventional trickle-bed reactors, monolithic reactors provide the advantages of low-pressure drop, large external surface areas and short diffusion lengths [1,2].

Carbon-coated monolithic ruthenium catalysts show high potential in the hydrogenation of D-glucose to D-sorbitol [3]. The preparation aspects and the obtained support properties of carbon-based monolithic structures are discussed in a review by Vergunst *et al.* [4]. However, hardly any knowledge is available on the application of an active phase to carbon-based monolithic structures (dispersion, distribution) and the accessibility and performance in liquid-phase operation [3,5]. Such knowledge would greatly facilitate the design and preparation of carbon-coated monolithic catalysts. Therefore, in this study the catalyst preparation process is investigated in detail, including (i) the impregnation of the monolithic supports with ruthenium and (ii) the dispersion and distribution of the active phase. Propositions will be made for the improvement of the distribution and dispersion of ruthenium on carbon-coated monolithic supports.

* To whom correspondence should be addressed.
E-mail: F.Kapteijn@tnw.tudelft.nl

2. Experimental

2.1. Catalyst preparation

Carbon-coated monolithic supports have been prepared according to a method developed by García-Bordejé *et al.* [6], starting from cordierite monolithic supports. Cordierite, a magnesium alumino-silicate with a melting point of about 1738 K, has a thermal expansion coefficient comparable to that of carbon, thereby increasing the stability of the formed composite [7]. The monoliths used in this study have square cells, a cell density of 62 cells cm^{-2} (400 cpsi) and a wall thickness of 0.18 mm. The samples had a length of 5 cm and a diameter of 1 cm.

Furan resin (Hüttenes–Albertus) was used as the carbon-yielding precursor. Polyethyleneglycol-4000, abbreviated to PEG-4000, was used as a pore former. In the initial step of the coating process, 20 cm^3 of Furan resin was mixed with 10 cm^3 of polyethyleneglycol-200 (dispersing agent) and 5 g of PEG-4000. 0.5 cm^3 of

1011-372X/03/1000–0181/0 © 2003 Plenum Publishing Corporation

concentrated nitric acid (65%) was used as the curing agent. The cordierite monoliths were dipcoated in the polymer mixture and allowed to soak for 3 min. After dipcoating, the excess solution was drained by several cycles of nitrogen blowing. The polymer is consolidated at room temperature overnight, after which the curing was completed at 363 K for a day. After complete consolidation, the coated substrates were heated with a rate of 10 K min^{-1} to 973 K in inert atmosphere (argon) for 2 h. These conditions were effective in converting the polymeric coatings into carbon. This procedure resulted in samples having a carbon load of ca. 8 wt%. The obtained carbon-coated monoliths were activated in CO_2 at 1123 K for 14 h in order to increase the specific surface area. This procedure resulted in a burn off of ca. 40%. Ruthenium was applied by impregnation with 0.2 g of $[RuCl_5 \cdot xH_2O]^{2-}$ in 80 g of diluted hydrochloric acid (0.01 M) under reflux conditions and continuous stirring (figure 1). The low pH was used to stay below the point of zero charge (PZC) of the carbon to create an electrostatic interaction between the carrier surface and the ruthenium complex. After 6.5 h, the monoliths were drained of the solution and excess liquid was blown out of the channels with pressurized air. The monoliths were carefully washed with demineralized water until the filtrate was pH neutral, followed by static air drying at room temperature and subsequently in an oven at 353 K. The catalysts were reduced under flowing hydrogen at 1 K min^{-1} from room temperature to 413 K, maintained at this temperature for 3 h and subsequently cooled under nitrogen. Finally, the catalysts were passivated by a mixture of 1% O_2 in nitrogen for 12 h at room temperature.

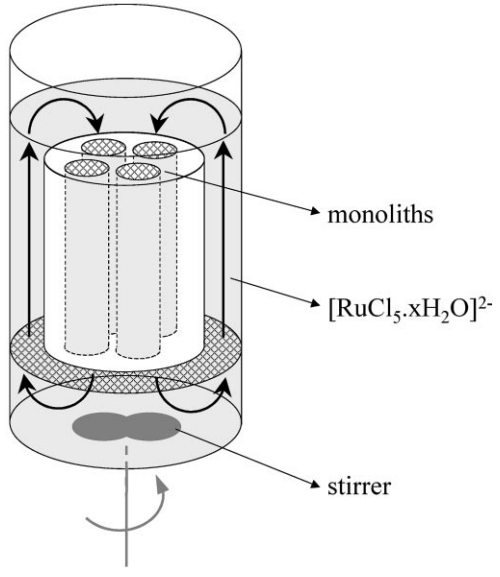

Figure 1. Schematic representation of the monolithic catalyst preparation setup, in which four pieces are loaded simultaneously.

2.2. Catalyst characterization

2.2.1. Volumetric nitrogen physisorption

Nitrogen physisorption measurements were performed at 77 K on a Quantachrome Autosorb 6B after degassing in vacuum at 623 K for 16 h. The specific surface area of the samples was determined from the adsorption isotherms by the BET theory. Calculations were performed in the relative pressure range 0.01–0.10 following standard ASTM D-4365, which is applicable to microporous materials. Using this technique, pore diameters in the region of 1.5–200 nm could be analyzed. The specific surface area and pore volume were calculated on the basis of the carbon content, rather than on the total mass, since the monolithic samples contained about 92 wt% ceramic material that showed no evidence of micro- or mesoporosity.

2.2.2. Volumetric hydrogen chemisorption

The active ruthenium surface area and dispersion of the monolithic catalysts were determined by volumetric hydrogen chemisorption. The pretreatment as well as the analysis was performed on the Quantachrome Autosorb-1C. Prior to analysis, the samples were dried in vacuum at 393 K. After drying, the passivated samples were reduced in hydrogen for 2 h at 393 K and evacuated at 393 K for 2 h. After cooling down in vacuum, the H_2 adsorption isotherms were measured at 308 K. The isotherm representing strong adsorption (back sorption method) was used to calculate the ruthenium surface area assuming a $Ru:H_2$ stoichiometry of 2 : 1 [8].

2.2.3. Transmission electron microscopy

Transmission electron microscopy (TEM) was performed using a Philips CM30T electron microscope with a LaB_6 filament as the source of electrons, operated at 300 kV. The carbon layer was scraped off the monolith by means of a scalpel. Samples were mounted on a microgrid carbon polymer supported on a copper grid by placing a few droplets of a suspension of ground sample in ethanol on the grid, followed by drying at ambient conditions.

2.2.4. Electron probe microanalysis (EPMA)

In order to obtain a flat cross section of the brittle monolithic structure, which is required for executing reliable and quantitative X-ray microanalysis, the sample material was moulded into the electrically conducting, methylmethacrylate-based resin Technovit 5000. This resin, after hardening, fills the channels of the monolithic structure and makes it possible to polish the sample, with good results. The surface of the sample has been successively ground, lapped, and polished. The final polishing step was performed with 1-μm diamond grains on a soft cloth. After each preparation step the sample was thoroughly cleaned ultrasonically in etha-

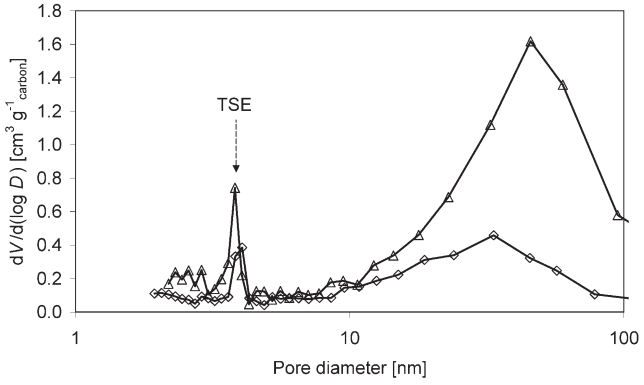

Figure 2. BJH pore-size distribution derived from the desorption branch of the nitrogen isotherm at 77 K: (◇) carbon-coated support, prior to CO_2-activation; (△) catalyst 0.4% Ru/C/cordierite.

nol. The samples were dried by blowing with pure nitrogen gas. The EPMA measurements were performed using a JEOL JXA 8900R microprobe using an electron beam with an energy of 15 keV and a current of 20 nA. The same equipment was used to record the scanning electron microscopy (SEM) images. The composition of the samples was determined quantitatively using the X-ray intensities, observed by wavelength dispersive spectrometry (WDS), of the constituent elements ruthenium, carbon and aluminium (cordierite is composed of $2MgO:5SiO_2:2Al_2O_3$), after background correction relative to the corresponding intensities of the reference materials. The intensity ratios thus obtained were processed with the matrix correction program CITZAF [9]. The counting errors for the spectral lines of ruthenium, carbon and aluminium used in the quantitative analysis amount to 0.23, 0.26, and 0.18 wt%, respectively. X-ray emission maps consisting of 250 × 250 points covering an area of approximately 150 × 150 μm were acquired. The recording time of each pixel was 800 ms.

Table 1
N_2-physisorption and hydrogen chemisorption results for the carbon-coated monolithic support, before CO_2-activation, and catalyst 0.4% Ru/C/cordierite

	Support	0.4% Ru/C/cordierite
Carbon loading [wt%]	8.4	4.9
S_{BET} [$m^2\ g^{-1}_{carbon}$]	500	860
V_{tot} [$cm^3\ g^{-1}_{carbon}$]	0.48	1.17
S_{micro} [$m^2\ g^{-1}_{carbon}$][a]	400	660
V_{micro} [$cm^3\ g^{-1}_{carbon}$][a]	0.16	0.27
$V_{meso/macro}$ [$cm^3\ g^{-1}_{carbon}$][b]	0.32	0.90
S_{Ru} [$m^2\ g^{-1}_{catalyst}$]		0.12
Metal dispersion [%]		7.1
d [nm]		18

[a]Determined by t-method micropore analysis.
[b]Determined in the pore diameter range of 2–200 nm.

3. Results

3.1. Texture

The N_2-physisorption results for the carbon-coated monolithic support, prior to CO_2-activation, and catalyst 0.4% Ru/C/cordierite, are given in table 1. Besides micropores, the carbonized carbon-coated monolithic support exhibits meso/macropores in the region of 10–100 nm (figure 2). The sharp peak at ~4 nm in the pore-size distribution derived from the N_2 desorption isotherm is an artifact attributed to the tensile strength effect (TSE) of the adsorbate [10]. At this stage, the carbon has a relatively low specific surface area compared to the common activated carbons with pores mainly in the micropore range. The texture was further developed by CO_2-activation. The 40% burn off resulted in an increase of the specific surface area from 500 to 860 $m^2\ g^{-1}_{carbon}$, while the total pore volume increased from 0.48 to 1.17 $cm^3\ g^{-1}_{carbon}$. The micropores are enlarged together with a progressive increase in the 10–100 nm pore-size range by CO_2-activation (figure 2).

3.2. Ruthenium surface area and particle size

The active ruthenium surface area of catalyst 0.4% Ru/C/cordierite was determined by volumetric hydrogen chemisorption to be 0.12 $m^2\ g^{-1}_{sample}$. This corresponds to an average ruthenium particle size of 18 nm and a dispersion of 7% (table 1). Figure 3 shows a representative TEM image of catalyst 0.4% Ru/C/cordierite. The ruthenium particles appear as dark dots on the surface of the carbon. The image shows that the ruthenium distribution was rather inhomogeneous. Some areas contained small ruthenium particles of ca. 1 nm (like those observed in case of the slurry catalyst prepared in a similar way [3]), while other areas

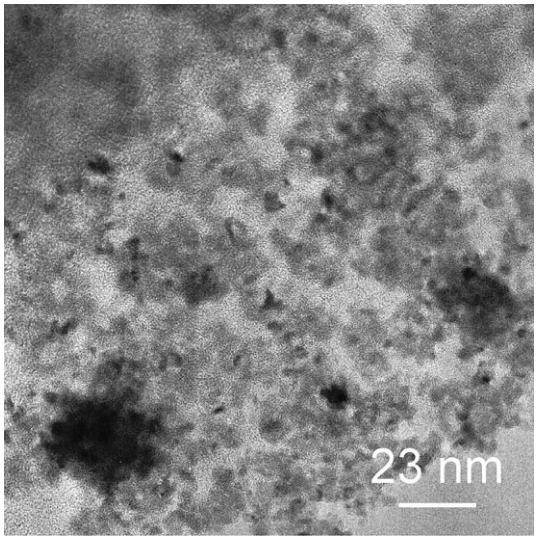

Figure 3. TEM image of the ruthenium on carbon-supported monolithic catalyst.

contained clusters of small or large ruthenium particles, resulting in the low dispersion.

3.3. Location of ruthenium in the monolithic catalyst

Figure 4 shows the backscattered electron image of a cross section of the carbon-coated monolithic ruthenium catalyst. It can be seen that the application of the carbon washcoat hardly affected the geometric surface properties of the monolithic support. More detailed information about the carbon distribution was obtained by EPMA analysis. Figure 5(a) shows that the carbon is situated primarily within the macroporous structure of the cordierite with only a thin layer on the external surface of the monolith channels. The red spots indicate the places where a relatively high amount of carbon is located. In the case of square cells, there is some carbon accumulation in the corners of the channels. The distribution of the ruthenium species on the carbon-coated monolithic catalyst is shown in figure 5(b). Ruthenium is not only present in the pores of the carbon washcoat layer but throughout the entire matrix. The bright spots indicate the places where a relatively high amount of ruthenium is present. To be able to discriminate whether the ruthenium species are preferentially located on the carbon inclusions or on the walls of the bare cordierite, the magnification was increased from 150 to 350×. EPMA maps of the area indicated by the white box in figure 4 for ruthenium, carbon, and aluminium (Al Kα emission image is not shown) were measured. These show that the ruthenium species are located at the accessible carbon surface, i.e., in the pores of the outer washcoat layer and on the edges of the carbon inclusions in the walls (figure 6). No ruthenium was detected inside the carbon inclusions, indicating that these inclusions were nonporous or not accessible to the impregnation liquid. No correlation between the ruthenium map and the corresponding map was found. Due to the resolution of the EPMA probe (about 1 μm), no information could be acquired concerning the metal particle size in the ruthenium domains.

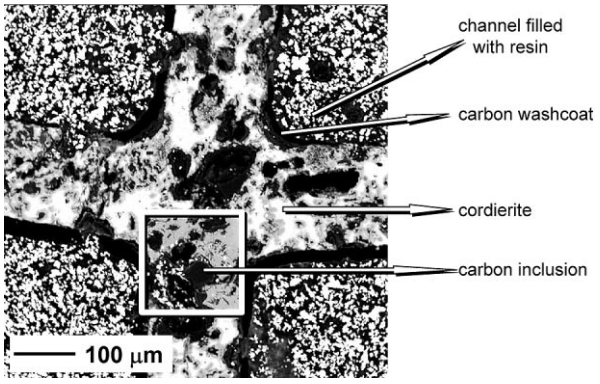

Figure 4. Backscattered SEM image of the 0.4% Ru/C/cordierite catalyst. The white box indicates the area shown in figure 6.

4. Discussion

The carbon-coated monolithic ruthenium catalyst showed a low dispersion and an inhomogeneous coverage of ruthenium. On the other hand, the slurry catalyst prepared in a similar way as the current 0.4% Ru/C/cordierite showed a homogeneous coverage with small ruthenium particles [3]. The ruthenium particle-size distribution for the slurry catalyst was very narrow. Immobilization of the $[RuCl_5]^{2-}$ complex, therefore, occurred via a strong adsorption on the carbon support. Principally, two types of strong adsorption sites are present on the carrier for the ruthenium complex, namely C=C structures in the carbon basal planes (π-complexation) and oxygen-containing functional groups to which the precursor can be anchored. Both the types of coordination would take place at the edges of the carbon basal plane structures [11]. Although the exact structures of the complexes could not be identified, it can be tentatively concluded that the ruthenium ions formed during the impregnation of the slurry carbon were bound at the basal plane edges. Owing to a different preparation procedure (carbon precursor, carbonization/activation conditions, etc.), the carbon-coated monolithic support contains a low amount of basal plane edges compared to the slurry support. As a consequence, part of the ruthenium precursor cannot be immobilized by means of strong adsorption, but only through weak physisorption forces. Accordingly, immobilization of this part of the ruthenium is to be effected by crystallization. Hence, the stage of drying in which crystallization proceeds is of great importance for the distribution of the active precursor within the final catalyst [12,13]. The broad pore-size distribution of the carbon-coated monolith can severely affect the migration of the metal during drying. Because, after washing, the micropores preferably remain filled with impregnation liquid because of the capillary forces (it is believed that the impregnation liquid in these micropores is only diluted upon washing), the liquid evaporates both from the small and wide pores and a net migration of the liquid from the wide meso- and macropores to these narrow pores will occur upon static drying. This migration will result in clusters of particles of the active precursor at the pore mouth openings. Thus, after primary crystallization, the growth of the nuclei will prevail over the formation of new nuclei, resulting in the low dispersion observed for the monolithic ruthenium catalysts. This macroscopic transport of the active-phase precursor upon drying has been demonstrated for the deposition of nickel on alumina-washcoated monoliths [13].

In order to prepare highly dispersed ruthenium monolithic catalysts by impregnation, the washing step should be omitted to prevent redistribution and partial loss of the ruthenium precursor. To solve maldistribution of ruthenium upon drying, solvent removal

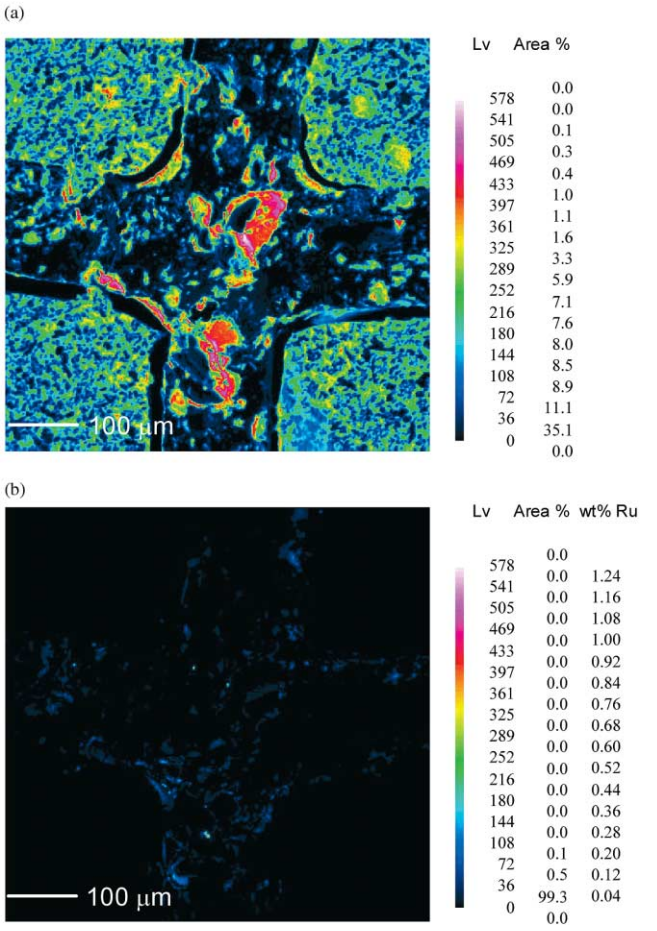

Figure 5. EPMA map at an intersection of the 0.4% Ru/C/cordierite catalyst. Figure (a) shows the C Kα emission image of the catalyst structure and (b) shows the Ru Lα emission image respectively (magnification 150×). The relative intensity of the elements corresponds with the level (Lv) indicated in the legend, accompanied by a specific color.

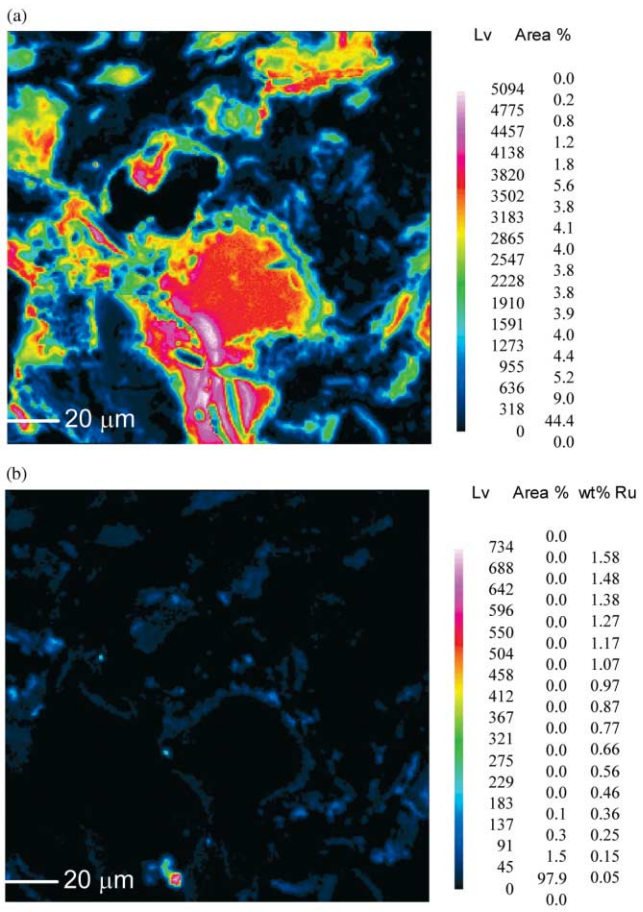

Figure 6. EPMA map on the 0.4% Ru/C/cordierite catalyst of the (a) carbon and (b) ruthenium distribution, respectively (magnification 350×).

techniques other than static air-drying, like freeze-drying or microwave drying, can be used [13]. By microwave drying, the heat is supplied homogeneously throughout the monolith structure, resulting in a more even drying. A problem arises when this way of drying is applied to large-sized monoliths because of the increased travel distance for the evaporated solvent to leave the monolith. If at one point in the monolith the gas becomes more saturated with solvent, the drying at this point will be slower and thus influences the ruthenium distribution [14]. To prevent the liquid from flowing to the exterior of the structure, freeze-drying can be applied. Although this technique yielded visually a more uniform metal distribution in the case of nickel supported on alumina-washcoated monoliths [13], it is not frequently applied in catalyst preparation due to the high expenses. Another way to slowdown the liquid movement is by increasing the liquid viscosity, e.g., by (i) adding glycerol or cellulose to water; (ii) changing the solvent; or (iii) using chelating ruthenium compounds [12]. Although this can improve the metal distribution, the presence of these compounds will also slowdown the drying rate.

An alternative method to apply ruthenium to the carbon-coated monolithic support is based on the formation of an insoluble complex by means of homogeneous deposition precipitation (HDP). Nickel on alumina-washcoated monoliths prepared by means of HDP showed visually a uniform active-phase distribution [13]. However, no data were provided regarding the dispersion and particle-size distribution. Toebes *et al.* [15] suggested that the presence of surface oxygen groups (SOC) on the carbon is essential for the deposition of ruthenium on carbon nanofibers according to the HDP method. The SOCs probably function as nucleation sites for precipitation and ensure good wetting properties of the surface for the aqueous solution of the metal precursor. The carbon-coated monolithic supports, therefore, need to be oxidized in diluted air after CO_2-activation to introduce SOCs.

The EPMA analyses showed that the ruthenium species are present both in the pores of the outer carbon washcoat layer and on the surface of the carbon inclusions located inside the monolith walls. No ruthenium was found in the empty macropores of the

cordierite, since (i) there is no strong interaction between the precursor and the cordierite and (ii) after impregnation and washing, the macropores are emptied first upon drying because of the capillary forces. The presence of an active phase in the walls of the monolithic substrate is undesired, since it makes the diffusion path of the reactants to the active ruthenium sites longer. To prevent deposition of ruthenium in the wall, (i) substrates with nonporous walls can be used or (ii) slurry coating can be applied, by which the coating layer is primarily deposited on the external surface of the monolith channels. To achieve this, a suspension of particles of similar size as the macropores in the cordierite (typically 5 μm) should be used [14]. For a more uniform thickness of the coating layer, rounded corners or round channels are preferred [16].

5. Conclusions

Carbon-coated monolithic supports have been prepared by dipcoating cordierite monoliths in a polymer mixture using Furan resin as the carbon-yielding precursor. A single dipcoating step resulted after carbonization in a carbon loading of ca. 8 wt%. The textural properties of the carbon washcoat layer have been optimized by CO_2-activation at 1123 K (40% burn off). The latter treatment resulted in an increase of the specific surface area from 500 to 860 $m^2\ g^{-1}_{carbon}$, while the total pore volume increased from 0.48 to 1.17 $cm^3\ g^{-1}_{carbon}$. Next to micropores, the resulting carbon displayed meso/macropores in the region of 10–100 nm. The active-phase loading was performed using a $[RuCl_5]^{2-}$ complex. Only part of this complex was immobilized by strong adsorption at the basal plane edges of the carbon coating. The rest of the ruthenium was bound through weak physisorption forces. This weak interaction between the metal precursor and support resulted in the migration of ruthenium upon drying due to capillary forces, resulting in an inhomogeneous ruthenium distribution with low dispersion. Owing to the macroporosity of the cordierite, the ruthenium species are not only present in the pores of the outer washcoat layer but also on the surface of the carbon inclusions inside the cordierite walls. Consequently, the diffusion paths to the active ruthenium sites are considerably larger than the average carbon-coating thickness, and the accessibility to the reactants is decreased. For the preparation of high-performance monolithic catalysts, the deposition of the active phase in the walls of the monolith should be prevented and the ruthenium complex should be immobilized. For a more uniform thickness of the coating layer, rounded corners or round channels are preferred.

Acknowledgment

Dr. Enrique García-Bordejé (Delft University of Technology) is acknowledged for preparing the carbon-coated monolithic supports. Corning USA generously supplied the ceramic monolithic substrates.

References

[1] F. Kapteijn, J.J. Heiszwolf, T.A. Nijhuis and J.A. Moulijn, CATTECH 3 (1999) 24.
[2] F. Kapteijn, T.A. Nijhuis, J.J. Heiszwolf and J.A. Moulijn, Catal. Today 66 (2001) 133.
[3] E. Crezee, B.W. Hoffer, P.R.M. Mooijman, B. van der Linden, J.C. Groen, M.L. Toebes, K.P. de Jong, F. Kapteijn and J.A. Moulijn, in preparation.
[4] Th. Vergunst, M.J.G. Linders, F. Kapteijn and J.A. Moulijn, Catal. Rev. 43 (2001) 291.
[5] Th. Vergunst, F. Kapteijn and J.A. Moulijn, Catal. Today 66 (2001) 381.
[6] E. García-Bordejé, F. Kapteijn and J.A. Moulijn, Carbon 40 (2002) 1079.
[7] E.M. DeLiso, K.P. Gadkaree, J.F. Mach and K.P. Streicher, US Patent 5,451,444 (1995).
[8] D.O. Uner, M. Pruski and T.S. King, J. Catal. 156 (1995) 60.
[9] J.T. Armstrong, in *Quantitative elemental analysis of individual microparticles with electron beam instruments*, K.F.J. Heinrich and D.E. Newbury (eds), (Plenum, New York, 1991), p. 261.
[10] J.C. Groen, J. Pérez-Ramírez and L.A.A. Peffer, Chem. Lett. 1 (2002) 94.
[11] H.E. van Dam and H. van Bekkum, J. Catal. 131 (1991) 335.
[12] P.J. van den Brink, *The Selective Oxidation of Hydrogen Sulfide to Elemental Sulfur on Supported Iron-based Catalysts*, Ph.D. Thesis (University of Utrecht, Utrecht, 1992).
[13] Th. Vergunst, F. Kapteijn and J.A. Moulijn, Appl. Catal. A: Gen. 213 (2001) 179.
[14] T.A. Nijhuis, A.E.W. Beers, Th. Vergunst, I. Hoek, F. Kapteijn and J.A. Moulijn, Catal. Rev. 43 (2001) 345.
[15] M.L. Toebes, F.F. Prinsloo, J.H. Bitter, A.J. van Dillen and K.P. de Jong, J. Catal. 214 (2003) 78.
[16] E. Crezee, C.S. Tjon Joen Sjong, F. Kapteijn and J.A. Moulijn, Carbon, submitted.